Article

Cell Chemical Biology

SIRT2- and NRF2-Targeting Thiazole-Containing Compound with Therapeutic Activity in Huntington's Disease Models

Highlights

- Novel thiazole-containing inhibitors of sirtuin-2 deacetylase identified
- Lead-compound is neuroprotective in Huntington's disease models
- Lead-compound is SIRT2-independent inducer of NRF2-dependent responses
- Novel NRF2 inducers reduce levels of reactive oxygen and nitrogen species

Authors

Luisa Quinti, Malcolm Casale, Sébastien Moniot, ..., Donald C. Lo, Leslie M. Thompson, Aleksey G. Kazantsev

Correspondence

akazantsev47@gmail.com

In Brief

There is currently no disease-modifying treatment for the neurodegenerative disorder Huntington's disease (HD). Quinti et al. identified a novel compound with therapeutic activity in HD models that has two distinct biochemical activities, highlighting the potential combinatorial therapeutic effect of this compound for drug development.

Quinti et al., 2016, Cell Chemical Biology *23*, 1–13
July 21, 2016
http://dx.doi.org/10.1016/j.chembiol.2016.05.015

CellPress

Please cite this article in press as: Quinti et al., SIRT2- and NRF2-Targeting Thiazole-Containing Compound with Therapeutic Activity in Huntington's Disease Models, Cell Chemical Biology (2016), http://dx.doi.org/10.1016/j.chembiol.2016.05.015

SIRT2- and NRF2-Targeting Thiazole-Containing Compound with Therapeutic Activity in Huntington's Disease Models

Luisa Quinti,[1,15] Malcolm Casale,[2,15] Sébastien Moniot,[3,15] Teresa F. Pais,[4] Michael J. Van Kanegan,[5] Linda S. Kaltenbach,[5] Judit Pallos,[6] Ryan G. Lim,[7] Sharadha Dayalan Naidu,[8] Heike Runne,[9] Lisa Meisel,[3] Nazifa Abdul Rauf,[1] Dmitriy Leyfer,[1] Michele M. Maxwell,[1] Eddine Saiah,[10] John E. Landers,[11] Ruth Luthi-Carter,[9] Ruben Abagyan,[12] Albena T. Dinkova-Kostova,[8,13] Clemens Steegborn,[3] J. Lawrence Marsh,[7] Donald C. Lo,[5] Leslie M. Thompson,[2,7,14] and Aleksey G. Kazantsev[1,*]

[1]Department of Neurology, Harvard Medical School and Massachusetts General Hospital, Boston, MA 02114, USA
[2]Department of Neurobiology and Behavior, University of California, Irvine, CA 92697, USA
[3]Department of Biochemistry, University of Bayreuth, 95447 Bayreuth, Germany
[4]Cell and Molecular Neuroscience Unit, Instituto de Medicina Molecular, Avenida Professor Egas Moniz, 1649-028 Lisbon, Portugal
[5]Department of Neurobiology, Center for Drug Discovery, Duke University Medical Center, Durham, NC 27710, USA
[6]Department of Developmental and Cell Biology
[7]Department of Biological Chemistry
University of California, Irvine, CA 92697, USA
[8]Division of Cancer Research, School of Medicine, University of Dundee, Dundee DD1 9SY, UK
[9]Functional Neurogenomics, Brain Mind Institute, Ecole Polytechnique Fédérale de Lausanne, 1015 Lausanne, Switzerland
[10]BioTherapeutics Chemistry, Pfizer Worldwide Medicinal Chemistry, 200 Cambridge Park Drive, Cambridge, MA 02140, USA
[11]Department of Neurology, University of Massachusetts Medical School, Worcester, MA 01655, USA
[12]Skaggs School of Pharmacy and Pharmaceutical Sciences, University of California, San Diego, CA 92093-0747, USA
[13]Departments of Medicine and Pharmacology and Molecular Sciences, Johns Hopkins University School of Medicine, Baltimore, MD 21205, USA
[14]Department of Psychiatry and Human Behavior, University of California, Irvine, CA 92697, USA
[15]Co-first author
*Correspondence: akazantsev47@gmail.com
http://dx.doi.org/10.1016/j.chembiol.2016.05.015

SUMMARY

There are currently no disease-modifying therapies for the neurodegenerative disorder Huntington's disease (HD). This study identified novel thiazole-containing inhibitors of the deacetylase sirtuin-2 (SIRT2) with neuroprotective activity in ex vivo brain slice and *Drosophila* models of HD. A systems biology approach revealed an additional SIRT2-independent property of the lead-compound, MIND4, as an inducer of cytoprotective NRF2 (nuclear factor-erythroid 2 p45-derived factor 2) activity. Structure-activity relationship studies further identified a potent NRF2 activator (MIND4-17) lacking SIRT2 inhibitory activity. MIND compounds induced NRF2 activation responses in neuronal and non-neuronal cells and reduced production of reactive oxygen species and nitrogen intermediates. These drug-like thiazole-containing compounds represent an exciting opportunity for development of multi-targeted agents with potentially synergistic therapeutic benefits in HD and related disorders.

INTRODUCTION

Mammalian NAD^+-dependent sirtuin deacetylases (SIRT1-SIRT7) regulate diverse physiological functions in cells and are implicated as potential modifiers of age-related human diseases (Liu et al., 2013). The second family member, sirtuin-2 (SIRT2), was originally identified as α-tubulin deacetylase (North et al., 2003). Later studies, however, indicated that SIRT2 deacetylates a broad variety of protein substrates and regulates multiple cellular processes, including histone remodeling and gene transcription (Rauh et al., 2013; Taylor et al., 2008). SIRT2 is a highly abundant protein in the adult CNS, including in neurons, although its precise function(s) remains uncertain (Luthi-Carter et al., 2010; Maxwell et al., 2011). We previously identified neuroprotective properties associated with several selective inhibitors of SIRT2 deacetylase (Chopra et al., 2012; Luthi-Carter et al., 2010; Outeiro et al., 2007).

Huntington's disease (HD), an autosomal dominant and progressive neurodegenerative disorder, is caused by expansion of a polymorphic trinucleotide repeat sequence $(CAG)_n$ within the gene encoding the large, highly conserved protein, Huntingtin (HTT; 1993). The expression of mutant HTT induces complex pathogenic mechanisms and alterations in multiple cellular pathways, including but not limited to protein misfolding and aggregation, transcriptional dysregulation, mitochondrial dysfunction, and elevation of reactive oxygen species (ROS). In particular, the harmful role of oxidative stress has been described in both HD patients and in experimental models (Browne and Beal, 2006; Sorolla et al., 2012), and is potentially due to the inherent sensitivity of neurons to an excess of ROS (Johri and Beal, 2012; Li et al., 2010; Moller, 2010; Quintanilla and Johnson, 2009; Tsunemi et al., 2012).

However, no single neurodegenerative mechanism has emerged as the predominant mechanism and this complex disease pathology challenges effective development of neurotherapies.

The initial goal of the present study was to identify a new scaffold(s) of potent and selective SIRT2 inhibitors and to assess the therapeutic potential of these compounds in models of neurodegenerative diseases (Chopra et al., 2012; Luthi-Carter et al., 2010; Outeiro et al., 2007; Pallos et al., 2008). We identified and characterized a novel structural scaffold MIND4, which transpired to contain compounds with dual SIRT2 inhibition and antioxidant NRF2 (nuclear factor-erythroid 2 p45-derived factor 2) activation properties.

RESULTS

Identification of a Lead Series of Novel SIRT2 Inhibitors

To identify novel SIRT2 inhibitors, a scaffold-hopping approach was taken. We used derivatives of 8-nitro-5-R-quinoline and 5-nitro-8-R-quinoline, previously identified as substructures of bioactive compounds, as starting templates to create an initial focused library for screening compound activities in biochemical acetylation assays with human recombinant SIRT2 protein (Outeiro et al., 2007). Compounds were screened at a single concentration (10 μM) in triplicate in biochemical SIRT2 assays and counter-screened against SIRT3 activity to assess target selectivity. Using iterative structure-activity chemical modifications to improve potency and selectivity, we identified compound 5-nitro-8-{[5-(phenoxymethyl)-4-phenyl-4H-1,2,4-triazol-3-yl]thio}quinoline, henceforth MIND4 (Figures 1A and 1B). In vitro activity tests of MIND4 showed selective concentration-dependent inhibition of human recombinant SIRT2 deacetylase activity (Figures 1C–1E). A structure-activity relationship study identified additional thiazole analogs with selective SIRT2 inhibition activity; however, with lower potency than the parent compound MIND4 (Figure 1G). Intriguingly, a close structural analog 5-nitro-2-{[5-(phenoxymethyl)-4-phenyl-4H-1,2,4-triazol-3-yl]thio}pyridine, henceforth MIND4-17 (Figure 1G), lacked any SIRT2 inhibition activity in the tested concentration range of 0.1–10 μM (Figure 1F).

Characterization of a Selective SIRT2 Inhibition Mechanism of the Lead Inhibitor MIND4

The precise potency of SIRT2 inhibition by MIND4 was determined as the half maximal inhibitory concentration (IC_{50}) = 1.2 ± 0.2 μM in a concentration-dependent activity test with human recombinant SIRT2 deacetylase (Figure 2A). A subsequent mechanistic study revealed competitive inhibition with NAD^+ and non-competitive inhibition with the peptide substrate with a K_i of 2.1 ± 0.2 μM (Figures 2B and 2C). We used these results and molecular docking to generate a model of a SIRT2/MIND4 complex, which defines a molecular basis for compound selectivity against SIRT2 (Figure 2D). The model shows partial MIND4 overlap with the NAD^+ binding site but not with the acetyl lysine site. Superimposition of the complex with SIRT1 and SIRT3 shows that MIND4 fits the larger SIRT2 active site. SIRT1 isoleucine-316 (Ile316) and SIRT3 leucine-395 (Leu395) and the corresponding helices would clash with MIND4, providing a rationale for SIRT2 selectivity.

Bioactivity of SIRT2 Inhibitor MIND4

The activity of MIND4 was tested in rat embryonic striatal ST14A cells stably expressing a 546 amino acid HTT fragment containing either a wild-type (26Q) or expanded (128Q) polyglutamine repeat (Ehrlich et al., 2001; Quinti et al., 2010). Consistent with the properties of a SIRT2 deacetylase inhibitor, MIND4 treatment increased acetylation of α-tubulin lysine-40 (K40) in both wild-type and HD cells (Figures 3A–3C) (North et al., 2003). Next, MIND4 activity was examined in wild-type primary cortical neurons (DIV11), which preferentially express full-length SIRT2 (isoform SIRT2.1) and are enriched in the brain SIRT2.2 isoform (Figure 3E) (Maxwell et al., 2011). Transient 6 hr treatment with MIND4 did not increase acetylation of cytoplasmic α-tubulin (K40), but upregulated acetylation of known nuclear H3 histone substrates lysine-56 and -27; acetylation levels of lysine-14 of H3 histone were unchanged (Rauh et al., 2013) (Figures 3E and 3F). An increase in histone acetylation suggests that such SIRT2 inhibition could influence gene transcription as reported in previous work (Luthi-Carter et al., 2010).

Treatment with MIND4 Is Neuroprotective in HD Models

Next, rat corticostriatal brain slice explants were used to test the neuroprotective potential of MIND4 in a complex neural tissue system expressing HTT exon 1 with expanded CAG repeats (mHTTex1) (Reinhart et al., 2011). Treatment with MIND4 significantly protected against mHTTex1-induced neurodegeneration in a concentration-dependent manner (Figure 3G). Neuroprotection at the highest 10 μM concentration of MIND4 was comparable with the efficacy of a reference compound, the pan-caspase inhibitor Boc-D-FMK (C) at 100 μM (Varma et al., 2007). MIND4 was further tested in an additional in vivo setting using a *Drosophila* model of HD, in which neuroprotective effects of SIRT2 inhibition has been established in previous studies (Marsh et al., 2003; Pallos et al., 2008). In this model, degeneration of photoreceptor neurons is visually scored by the presence of surviving rhabdomeres in the eyes of *Drosophila* expressing mHTTex1 (Steffan et al., 2001). Flies treated with 10 μM MIND4 had significantly more surviving rhabdomeres than untreated controls (Figure 3H). The neuroprotective effects of MIND4 were confirmed in an independent second trial conducted at the 10 μM dose (data not shown). Relative rescue was estimated as 22.6% and 20.7% for the first and second trials, respectively.

MIND4 Induces Transcriptional Activation of the NRF2 Pathway in HD and Wild-Type Neuronal Cells

We then sought to determine whether MIND4 treatment could alter gene expression, possibly restoring or compensating for transcriptional dysregulation in HD models as a possible neuroprotective mechanism (Crook and Housman, 2011; Luthi-Carter et al., 2002, 2010). We thus performed gene expression profiling to determine the impact of MIND4 on transcriptional readouts in wild-type and HD ST14A cells.

Mutant HD and wild-type ST14A cells (Ehrlich et al., 2001; Quinti et al., 2010) were treated with MIND4 at 5 μM for 24 hr. RNA from MIND4-treated and untreated HD mutant and wild-type ST14A cells was extracted and run on Affymetrix rat microarrays (Affy GeneChip Rat Genome 230 2.0 array) (http://www.ncbi.nlm.nih.gov/geo/query/acc.cgi?acc=GSE49392). Duplicates for each experimental condition were imported into Partek

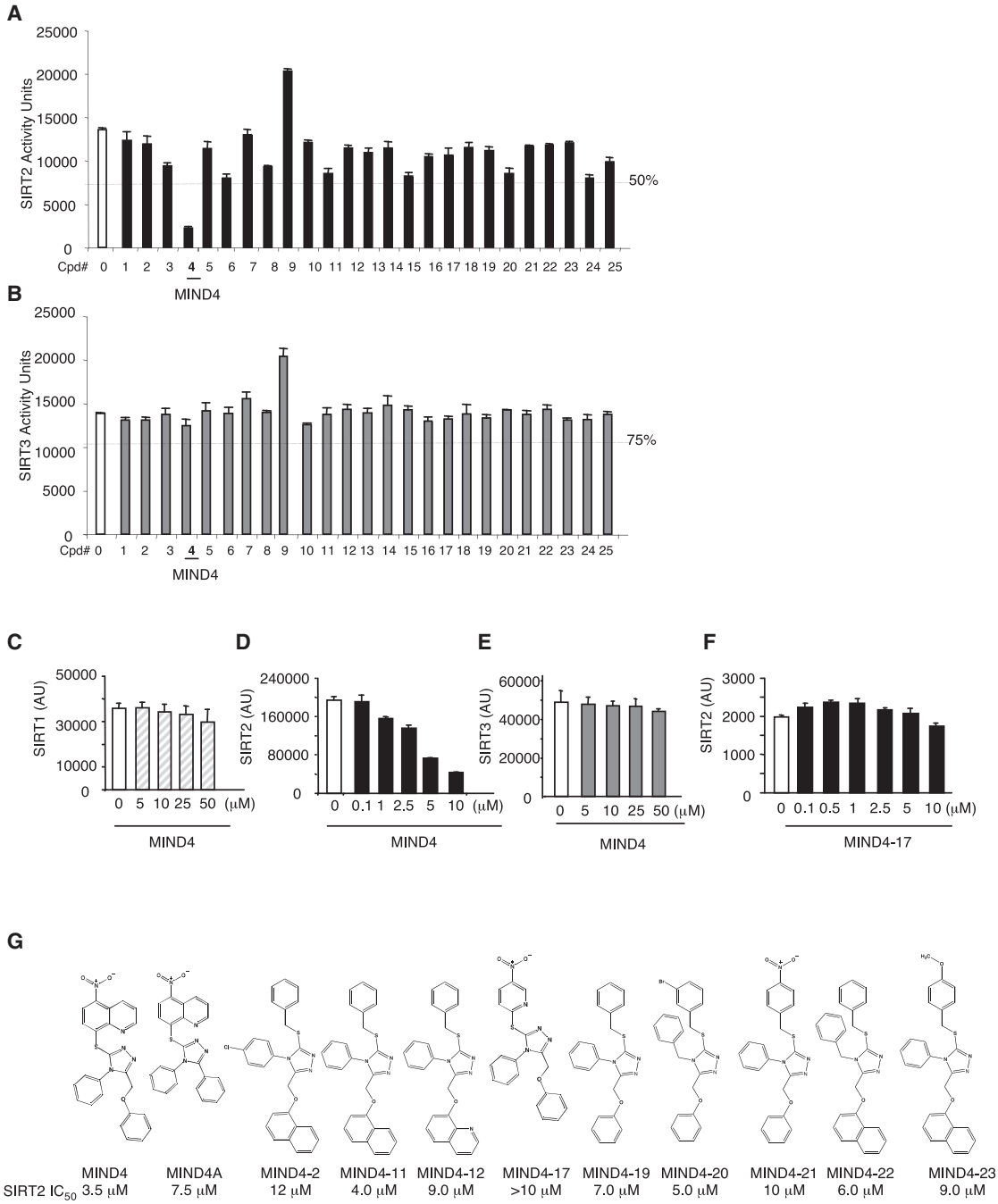

Figure 1. Identification of Potent and Selective SIRT2 Inhibitor MIND4

(A and B) Primary and counter screening of a focused library of 8-nitro-5-R-quinoline and 5-nitro-8-R-quinoline derivatives using SIRT2 (A) and SIRT3 (B) biochemical deacetylation assays. Compounds were screened at a single 10 μM concentration in triplicate. Selection of active inhibitors was set at the indicated threshold (dotted lines) of <50% of SIRT2 remaining activity; >75% of SIRT3 remaining activity. MIND4 (compound no. 4) was preliminary identified as a potent selective SIRT2 inhibitor.

(C–E) Concentration-response tests in SIRT1 (C), SIRT2 (D), and SIRT3 (E) biochemical deacetylation assays showed a selective inhibition of SIRT2 by MIND4.

(F) Concentration-response activity test showed no detectable SIRT2 inhibition activity of the structural analog MIND4-17.

(G) Structures and SIRT2 inhibition activities of MIND4 analogs. Compound SIRT2 IC_{50} values were established in concentration-response tests in vitro.

Genome Suite for biostatistical analysis. Genes showing significant differential expression were identified by ANOVA for three contrasts resulting in three gene lists: mutant HD (MT) versus wild-type (WT) = case I (disease phenotype); MT/MIND4 treated versus WT = case II (treatment phenotype); and MT/MIND4 treated versus MT = case III (mutant drug-dependent phenotype)

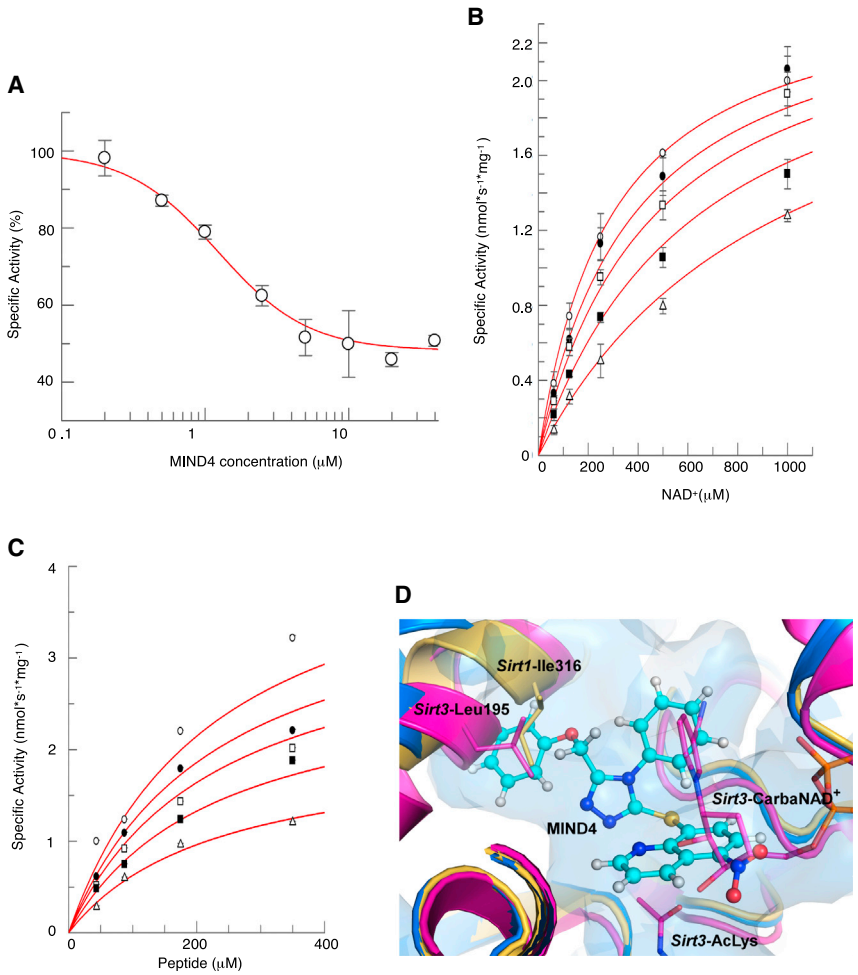

Figure 2. MIND4 Mechanism of SIRT2 Inhibition

(A) Concentration-dependent inhibition of SIRT2 activity by MIND4.

(B and C) Competition of MIND4 with the SIRT2 co-substrate NAD^+ and with acetylated substrate, respectively. Deacetylase activity of SIRT2 was measured at several MIND4 concentrations: 0 μM (empty circles), 0.625 μM (filled circles), 1.2 μM (empty squares), 2.5 μM (filled squares), and 5 μM (triangles). Reactions were conducted at increasing concentrations of NAD^+ (B) or peptide substrate (C). The best-fitting inhibition model is competitive for NAD^+ and non-competitive for the peptide substrate.

(D) Docking model of the SIRT2/MIND4 complex rationalizes isoform-selective inhibition. Overlaid structures of SIRT1 (yellow) (PDB: 4KXQ), SIRT2 (blue) (PDB: 3ZGV), and SIRT3 (pink) (PDB: 4FVT) are presented as cartoons. MIND4, docked in SIRT2, is shown as balls-and-sticks in light blue. Acetylated lysine peptide and non-hydrolyzable NAD^+ analog (carba-NAD^+), shown SIRT3-bound, are presented as pink sticks. The large SIRT2 active site cavity is displayed as a transparent blue surface.

(Table 1). These represented transcriptional alterations in MT cells compared with WT cells (case I), in MT treated cells compared with WT cells (case II), and in MT treated cells compared to untreated MT cells (case III). The lists, cases I–III, were then imported into Ingenuity Pathway Analysis (IPA; Ingenuity Systems, www.ingenuity.com) for pathway and network analyses.

Surprisingly, in treated MT cells compared with untreated MT cells (case III), all top seven of the most significant canonical pathways activated by MIND4 treatment were either directly or indirectly related to NRF2; in decreasing order of significance, these were: (1) the NRF2-mediated oxidative stress response itself, (2) glutathione-mediated detoxification, (3) lipopolysaccharide (LPS)/interleukin-1 (IL-1)-mediated inhibition of retinoid X receptor (RXR) function, (4) aryl hydrocarbon receptor signaling, (5) xenobiotic metabolism signaling, (6) glutathione redox reactions, and (7) glutathione biosynthesis (Figure 4A; please see Discussion for more details). Figure 4B shows a portion of the IPA canonical pathway of NRF2 colored by intensity correlated to fold-change of gene expression in treated versus untreated MT cells.

Next we tested whether MIND4 could also induce transcription of antioxidant response element (ARE) genes in primary neurons. WT rat primary striatal neurons were treated with MIND4 at a 5 μM dose for 24 hr and subjected to transcriptional microarray analysis as described (Luthi-Carter et al., 2010). The analysis of transcriptional changes shows that treatment with MIND4 induced a robust expression of canonical NRF2 gene targets in primary neurons as well (Table S1, Supplemental Experimental Procedures).

These results suggested the intriguing possibility that MIND4 is an inducer of NRF2, acting through a SIRT2 inhibition-dependent or -independent mechanism.

MIND4 Induces NRF2 Activation Response in an SIRT2-Independent Manner

To validate the transcriptional microarray data, WT and mutant HD ST14A cells were treated with MIND4 for 24 hr, and the expression levels of two canonical NRF2-responsive proteins, NQO1 and GCLM, were examined. Concentration-dependent increases in these proteins were observed in both cell lines, consistent with activation of NRF2 (Figures 5A and 5B).

Next, we examined the effects of MIND4 on the stabilization of NRF2 protein, a well-known step in the cascade of pathway activation. The effects of MIND4 on NRF2 levels were compared with the reference NRF2-inducer sulforaphane (SFP) (Zhang et al., 1992). Compounds were tested in COS1 cells transfected with plasmid constructs encoding NRF2-V5 proteins and β-galactosidase to normalize transfection efficiency between samples as previously described (McMahon et al., 2010). Treatment with both compounds resulted in stabilization of NRF2, as determined by the clear increases in protein levels (Figure 5C). These results further support the finding that MIND4 is an inducer of the NRF2 pathway.

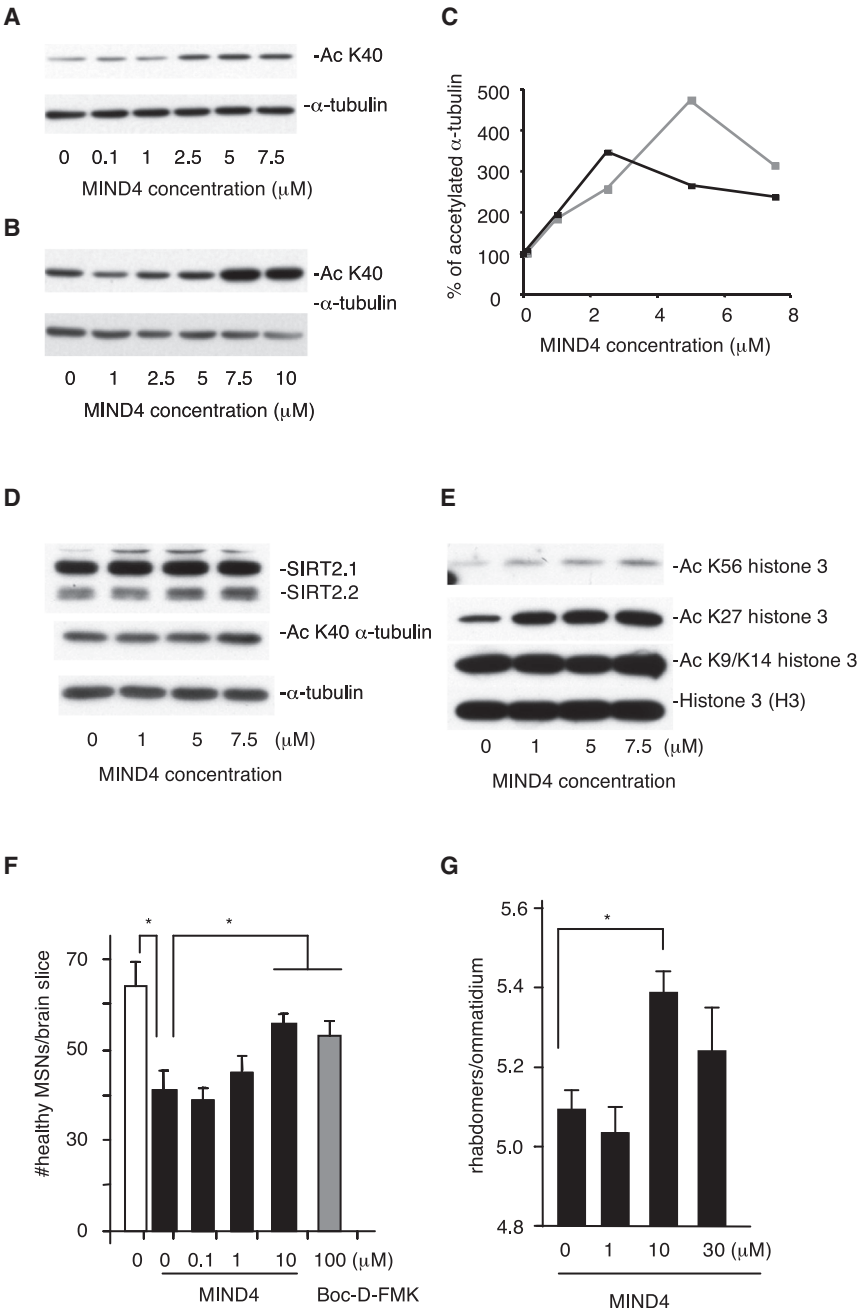

Figure 3. Bioactivity and Neuroprotective Properties of MIND4

(A and B) MIND4 treatment increases acetylation of α-tubulin lysine-40 (K40) in wild-type (A) and HD mutant (B) rat embryonic ST14A cells. Cells were treated with the compound for 6 hr, then the lysates were prepared and resolved by SDS-PAGE, and immunoblotted with antibodies specific to acetylated K40 and total α-tubulin.

(C) Quantification of α-tubulin acetylation from (A) and (B). Ratio of acetylated/total α-tubulin in wild-type (black line) and mutant HD (gray lane) was plotted against compound concentration.

(D and E) Effects of MIND4 on increase acetylation of SIRT2 substrates, cytoplasmic α-tubulin, and histone 3 (H3), in wild-type primary cortical mouse neurons (DIV 11) treated with the compound for 6 hr; protein levels were analyzed by immunoblotting with the respective antibodies. (D) Effects of MIND4 on acetylation of α-tubulin K40. Total α-tubulin levels were used as a loading control. A putative compound target is preferentially expressed as a full-length SIRT2 protein (SIRT2.1 isoform). (E) Effects of MIND4 on acetylation of H3 lysine-56 (K56), lysine-27 (K27), lysine-9, and lysine-14 (K9/K14). Total H3 levels were used as a loading control.

(F) MIND4 treatment protects medium spiny neurons (MSNs) in rat ex vivo brain slices against toxicity of a transiently transfected mutant (73Q) N terminus HTT fragment (mHTTex1). Yellow fluorescent protein (YFP) was used as a neuronal viability marker and co-transfected with mHTTex1 constructs (black bars). Effects are compared with the survival of neurons expressing the YFP plasmid alone (open bar) and expressed as the number of healthy YFP-positive MSNs per brain slice. MIND4 at the indicated concentrations (black bars) and the positive control pan-caspase inhibitor Boc-D-FMK at 100 μM (gray bar) were added directly to the tissue culture media. A statistically significant effect of MIND4 treatment was observed at 10 μM by ANOVA, followed by Dunnett's post hoc comparison test at the $p < 0.05$ confidence level.

(G) MIND4 enhanced survival of photoreceptor neurons in a *Drosophila* model of HD. Relative rescue of photoreceptor neurons, expressing the mutant HTTex1 fragment, in flies treated versus untreated with MIND4 at the10 μM dose was estimated as 22.6%.

*$p < 0.001$.

Treatment with the structural analog MIND4-11, also a SIRT2 inhibitor (IC_{50} = 4 μM), had no effect on induction of the NRF2 response (Figure 5D), further supporting a SIRT2-independent mechanism of NRF2 activation for MIND4. In contrast, treatment with the close structural analog MIND4-17, lacking SIRT2 inhibition activity, led to an even more potent induction of the NRF2-responsive proteins NQO1 and GCLM compared with MIND4 in both WT and HD mutant ST14A cells (Figures 5E and 5F). Together, the findings suggest that the parent compound MIND4 is also an inducer of NRF2, activating this pathway via a SIRT2 inhibition-independent mechanism.

Thiazole Analogs MIND4 and MIND4-17 Induce an NRF2 Activation Response in Primary Mouse Neurons and Astroglia

To extend evaluation of the NRF2 activation properties of MIND4 and MIND4-17 analogs, compound effects were tested in primary mouse neurons. A concentration-dependent induction of NQO1 and GCLM proteins in WT mouse cortical neurons (6 DIV) treated with MIND4-17 for 24 hr supported a direct induction of the NRF2 pathway (Figure 6G). These results showed that treatment with MIND4-17 can induce canonical NRF2 activation responses in mouse neurons.

Please cite this article in press as: Quinti et al., SIRT2- and NRF2-Targeting Thiazole-Containing Compound with Therapeutic Activity in Huntington's Disease Models, Cell Chemical Biology (2016), http://dx.doi.org/10.1016/j.chembiol.2016.05.015

Table 1. Gene Expression Analysis of MIND4-Treated Cells

Biochemical Pathways	Case I	Case II	Case III
NRF2-meditated oxidative stress response pathway	*ACTA2 ACTC1 CAT GSTA4 DNAJA1 KRAS MAF PRKCZ SOD2* *FOSL1 GSTA3 GSTT2/GSTT2B DNAJB12 JUNB DNAJC15 DNAJC14 PRKCH ENC1 DNAJC21*	*ABCC4 HMOX1 ACTA2 AOX1 KEAP1 CAT KRAS DNAJA1 MAFF DNAJA4 MGST1 MGST2 GCLC NQO1 GCLM PIK3CD GSR PRKCD GSTA2 GSTA3 PRKCZ GSTA4 SOD2 GSTM1 SQSTM1 GSTP1 TXNRD1* *JUNB DNAJC15 FOSL1 MGST3 PRKCH*	*ABCC4 GSTP1 AOX1 GSTT2/GSTT2B CAT HERPUD1 DNAJA4 HMOX1 DNAJB9 KEAP1 FOSL1 MAFF GCLC MGST1 GCLM MGST2 GSR NQO1 GSTA3 SQSTM1 GSTM5 TXNRD1*
Glutathione-mediated detoxification	*GSTA4* *GGH GSTA3 GSTT2/GSTT2B*	*GSTA2 GSTA3 GSTA4 GSTM1 GSTP1 MGST1 MGST2* *MGST3*	*GGH GSTA3 GSTA4 GSTM5 GSTP1 GSTT2/ GSTT2B MGST1 MGST2*
LPS/IL-1 mediated inhibition of RXR function	*ACOX1 GSTA4 ALDH1A2 ALDH1L2 ALDH3A1 IL33 ALDH6A1 MAOA CAT NR1H3 CPT1C FABP5* *GSTT2/GSTT2B ALDH1A3 HMGCS1 ALDH1L1 HS3ST1 HS3ST6 IL1RL1 ALDH9A1 NGFR CD14 PAPSS2 RXRA GSTA3 SLC27A3*	*ABCA1 GSTA2 ABCC3 GSTA3 ABCC4 GSTA4 ABCG1 GSTM1 ACOX1 GSTP1 ALAS1 ALDH1A2 IL1R2 ALDH1L2 MAOA ALDH3A1 MGST1 MGST2 CAT NR1H3 CPT1B CPT1C FABP5* *HMGCS1 HS3ST1 ALDH1A3 HS3ST6 ALDH1L1 ALDH9A1 MGST3 CD14 NGFR CHST2 PAPSS2 SLC27A3*	*ABCB1 GSTM5 ABCC4 GSTP1 ABCG1 GSTT2/ GSTT2B ALAS1 CAT IL1RL1 MAOA CPT1A MGST1 GSTA3 MGST2* *HMGCS1 CHST2 SULT1A3/SULT1A4*
Aryl hydrocarbon receptor signaling	*ALDH1A2 HSPB1 IL6 ALDH1L2 NFIA ALDH3A1 NFIC ALDH6A1 RARB RARG CYP1A1 GSTA4 TGFB3* *ALDH1A3 ALDH1L1 MYC NR2F1 ALDH9A1 CCND1 RXRA FAS RXRB GSTA3 SRC TGFB2 GSTT2/GSTT2B*	*ALDH1A2 GSTM1 GSTP1 HSPB1 ALDH1L2 IL6 ALDH3A1 MGST1 MGST2 NFIA NQO1 CYP1A1 CYP1B1 RARB GSTA2 RARG GSTA3 GSTA4 TGFB3* *ALDH1A3 ALDH1L1 ALDH9A1 APAF1 MGST3 CCND1 CCND3 NR2F1 RXRB*	*CYP1A1 GSTT2/GSTT2B CYP1B1 IL6 FAS MGST1 GSTA3 MGST2 GSTM5 MYC GSTP1 NQO1 NFIB*
Xenobiotic metabolism signaling	*ALDH1A2 GSTA4 ALDH1L2 ALDH3A1 IL6 ALDH6A1 KRAS MAF MAOA CAT MAP3K3 PPP2CB CYP1A1 PRKCZ* *ALDH1A3 GSTT2/GSTT2B ALDH1L1 HS3ST1 HS3ST6 ALDH9A1 CAMK2B CITED2 PPP2R2B GRIP1 PRKCH GSTA3 RXRA*	*ABCC3 HMOX1 ALDH1A2 IL6 ALDH1L2 KEAP1 ALDH3A1 KRAS MAOA MGST1 CAT MGST2 CYP1A1 NQO1 CYP1B1 PIK3CD GCLC PPP2CB GSTA2 GSTA3 PRKCD GSTA4 GSTM1 PRKCZ GSTP1 UGT1A1* *HS3ST1 ALDH1A3 HS3ST6 ALDH1L1 ALDH9A1 CAMK2B CHST2 MGST3 PPM1L GRIP1 PPP2R2B PRKCH*	*ABCB1 GSTT2/GSTT2B CAT HMOX1 IL6 CYP1A1 KEAP1 CYP1B1* *MAOA GCLC MGST1 GSTA3 MGST2 GSTM5 NQO1 GSTP1* *CHST2 SULT1A3/SULT1A4*
Glutathione redox reactions I		*PX7 GSR MGST1 MGST2* *GPX8 GPX1 MGST3*	*GSR MGST1 MGST2* *GPX1*
Glutathione biosynthesis		*GCLC GCLM*	*GCLC GCLM*

Statistically significant expression changes of genes for cases I–III: genes that are underlined are upregulated; genes not underlined are downregulated. The top seven canonical pathways are shown based on significance calculated by IPA for case III (MIND4-treated cells). Note that in case III transcripts were predominately upregulated.

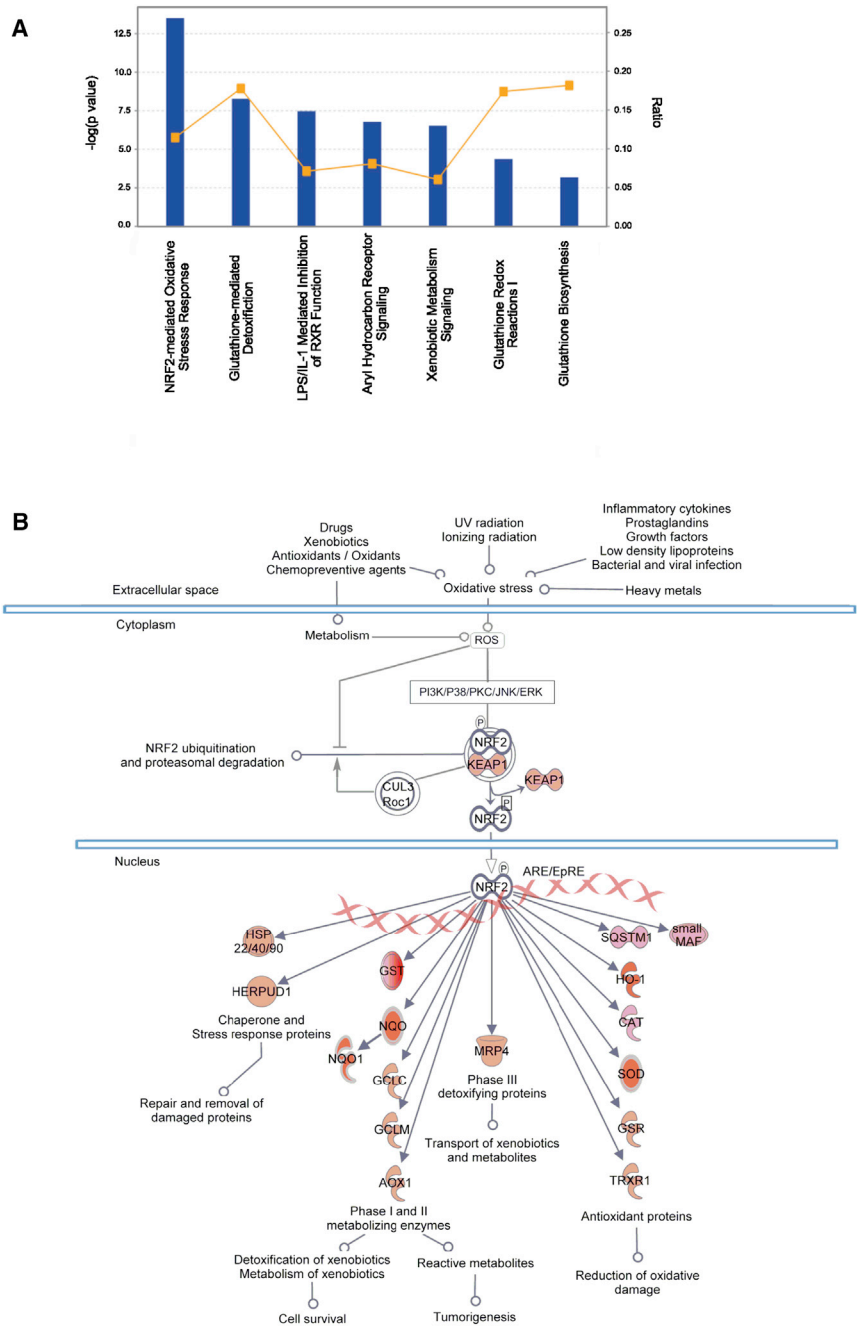

Figure 4. Gene Expression Profile and IPA Analysis

Gene expression profiling and IPA analysis revealed NRF2 as the major pathway impacted by MIND4 in mutant HTT-expressing cells (case III).

(A) Pathway analysis resulted in lists of IPA "canonical pathways," sorted according to Fisher's exact test right-tailed p value. The top canonical pathway was the NRF2-mediated oxidative stress response. This pathway had a highly significant log(p value) = 13.496. Other pathways are shown in decreasing order of significance to the right. The orange boxes are the ratios of the number of MIND4-affected genes in the pathway to the total number in the pathway.

(B) In case III, a fold-change increase of expression of NRF2-responsive genes is shown as a function of color intensity. Large changes are shaded with dark red, and decreasing values are shown in lighter red. The pathway shows differential expression in NRF2 downstream targets in mutant HTT-expressing cells in the presence and absence of MIND4.

We then examined whether MIND4-17, similarly to MIND4, could mediate transcriptional activation of canonical NRF2-responsive ARE genes. To that end we first used an ARE response element transcriptional reporter assay in a rat corticostriatal neuronal co-culture system (Kaltenbach et al., 2010). As shown in Figure 5H, MIND4-17 significantly increased the transcriptional rate of a 5×-ARE-luciferase reporter construct transiently transfected into corticostriatal co-cultures. As would be expected for direct activation of NRF2, an almost saturating transcriptional response was already observed within 4 hr of compound treatment.

Next, we determined whether MIND4-17 activates downstream ARE-dependent transcription of endogenous NRF2-target genes in native corticostriatal co-cultures. Treatment with MIND4-17 for 6 hr significantly and concentration-dependently increased the expression of the canonical ARE genes *Nqo1* (GenBank: NM_008706), *Hmox1* (GenBank: NM_010442), *Srx1* (GenBank: NM_029688), and to a lesser degree *Gclc* (GenBank: NM_010295) (Figures 5I–5L). These same genes were activated in primary rat neuronal cultures by MIND4 (Table S1). Finally, we compared the effects of MIND4 and MIND4-17 on transcriptional activation of the NRF2 pathway in the context of the HD mutation (Figures 5M and 5N). Both compounds showed similar concentration-dependent activation of the 5×-ARE-luciferase reporter in corticostriatal co-cultures derived from WT versus an HD mutant knockin mouse model (Q175/+) (Menalled et al., 2012). Treatment of cultures with MIND4-17 for 24 hr was not significantly cytotoxic for striatal (5 DIV) or cortical (5 DIV) neurons, differentially labeled in co-culture (Figure S1).

To extend the validation of NRF2 activation properties in non-neuronal cells, we tested MIND4 and MIND4-17 in primary mouse astroglia. Treatment with both compounds resulted in concentration-dependent increases of NRF2-responsive NQO1 and GCLM protein levels, demonstrating that the effects of these inducers are not restricted to neuronal cells (Figures 5O and 5P).

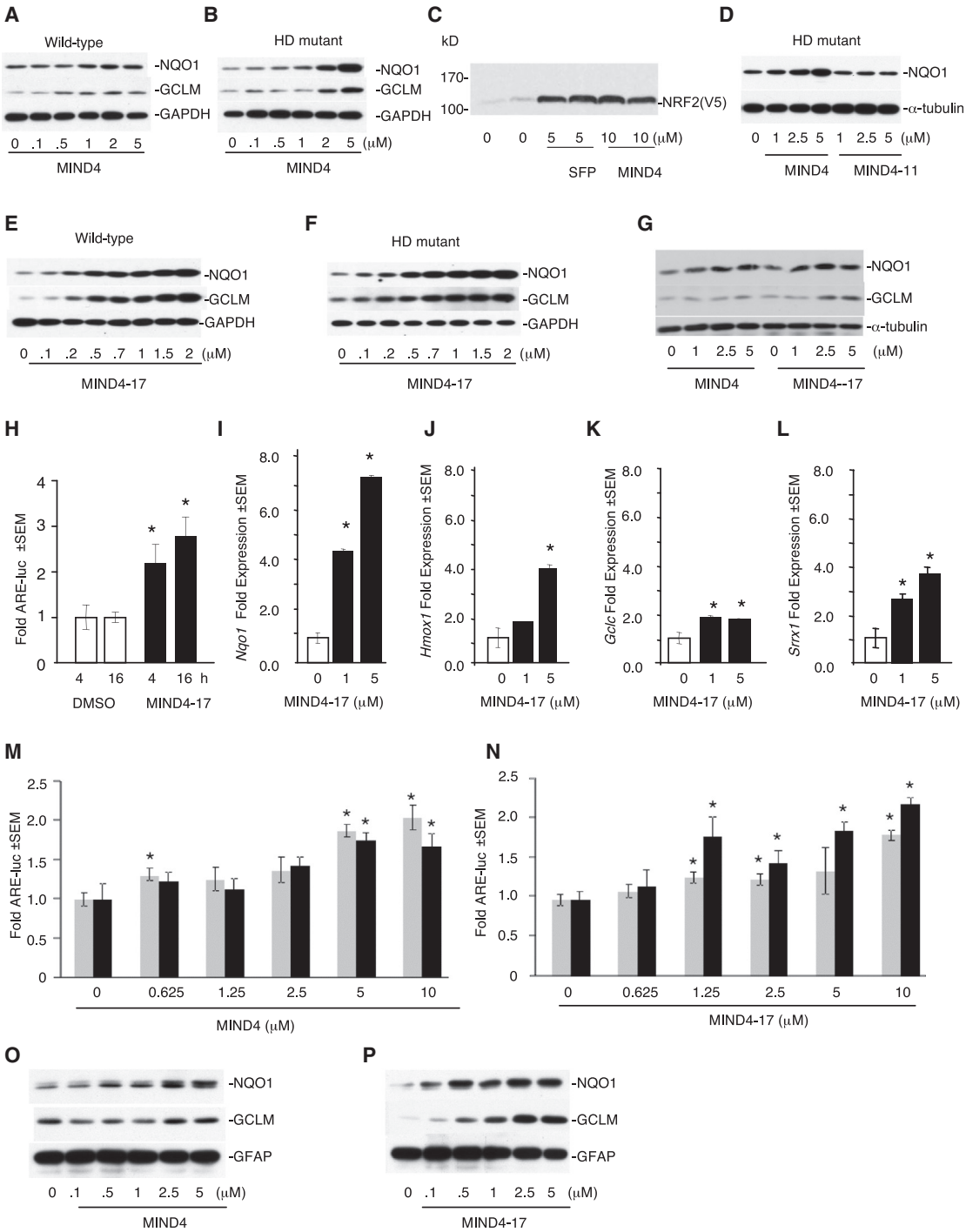

Figure 5. NRF2 Activation Properties of Thiazole Analogs MIND4 and MIND4-17

(A and B) Treatment with MIND4 increased expression of NRF2-responsive proteins NQO1 and GCLM in wild-type (A) and in HD mutant (B) rat embryonic ST14A cells. Levels of GAPDH were used as a loading control.

(C) Treatment with MIND4 increased the stability of NRF2. COS1 cells were co-transfected with plasmids encoding NRF2-V5, KEAP1, and β-galactosidase to monitor transfection efficiencies, and treated for 24 hr with MIND4 at 10 μM or the classical NRF2 inducer sulforaphane (SFP) at 5 μM. Cell extracts were prepared, proteins were resolved on SDS-PAGE, and NRF2 levels were detected by immunoblotting with a V5 antibody.

(D) Comparative analysis of NRF2 activation response of NQO1 expression by the SIRT2 inhibitors MIND4 and MIND4-11 in HD mutant ST14A cells. Cells were exposed to compounds for 24 hr. Levels of α-tubulin were used as a loading control.

(E and F) Treatment with MIND4-17 for 24 hr increased expression of the NRF2-responsive proteins NQO1 and GCLM in wild-type (E) and in HD mutant (F) ST14A cells. Levels of GAPDH were used as a loading control.

(legend continued on next page)

NRF2 Inducer MIND4 and Its Structural Analog MIN4-17 Reduce ROS Levels in Microglia

We next performed functional studies evaluating properties of MIND4 and MIND4-17 in a well-characterized microglia model of NRF2 activation (Innamorato et al., 2008; Koh et al., 2011) using lentiviral transduction of SIRT2 shRNA or a scrambled control (Figure 6A). The effects of both compounds on the levels of ROS were examined in microglia activated with LPS/tumor necrosis factor alpha (TNFα) as previously described (Pais et al., 2013). Treatment with MIND4 or MIND4-17 resulted in a decrease of ROS levels in WT microglia (Figure 6B), Notably, the effect of MIND4-17 was more pronounced than the effect of MIND4 and in agreement with the difference in inducer potencies of NRF2 activation. SIRT2 knockdown in microglia caused a significant elevation of ROS levels as previously described (Figures 6B and 6C) (Pais et al., 2013). Nonetheless, treatment with MIND4-17 was still able to decrease ROS levels, albeit with lower magnitude than in WT microglia (Figure 6C). The effects of MIND4 treatment on ROS levels were undetectable and likely due to its lower potency of NRF2 activation.

Since SIRT2 knockdown led to an increase, not a decrease, in ROS levels in microglia (Pais et al., 2013), SIRT2 inhibitory activity of MIND4 is presumably irrelevant for the observed antioxidant effects of MIND4 in WT microglia. Moreover, the antioxidant effects of MIND4-17 in WT and SIRT2-null microglia are clearly independent from SIRT2 since this compound lacks SIRT2 inhibitory activity. Together, these findings indicate that the antioxidant effects of both MIND4 and MIND4-17 are attributable to the NRF2-activating properties of these compounds.

NRF2 Inducers MIND4 and MIND4-17 Reduce Levels of Reactive Nitrogen Intermediates in Microglia

Finally, we examined whether induction of NRF2 through a SIRT2-independent mechanism could inhibit release of neurotoxic nitric oxide, produced by inducible nitric oxide synthase (iNOS) in activated microglia (Aguilera et al., 2007). Treatment with MIND4 and MIND4-17 reduced production of nitric oxide in a concentration-dependent manner in activated microglia, where the effect of MIND4-17 was again more pronounced (Figure 6D). The reduction of nitric oxide levels was similar in control cells (white bars) versus those transduced with SIRT2 shRNA (black bars), and irrespective of the presence or absence of SIRT2 inhibitory activity in MIND4 versus MIND4-17, respectively. These results were again consistent with a SIRT2-independent mechanism for NRF2 activation, here resulting in the reduction of nitric oxide levels in activated microglia.

DISCUSSION

We have identified a novel scaffold of thiazole-containing compounds which exhibits selective SIRT2-inhibition activity at various potencies. Mechanistic studies with the most potent compound elucidated an NAD^+-competitive mechanism of SIRT2 inhibition. MIND4 acts as a bioactive SIRT2 inhibitor, and is neuroprotective in ex vivo brain slice and in vivo *Drosophila* models of HD. Through a systems biology approach, we unexpectedly found that MIND4 is also a transcriptional inducer of the NRF2-mediated oxidative stress response and modulates multiple pathways (see Figure 4A), all centrally regulated byNRF2 activation: in glutathione-mediated detoxification, NRF2 regulates the expression of multiple members of the glutathione S-transferase supergene superfamily, the enzymes that catalyze the conjugation of numerous xenobiotics with glutathione (Hayes and Dinkova-Kostova, 2014; Wu et al., 2012). In LPS/IL-1 mediated inhibition of RXR function, NRF2 binds directly to RXR through its Neh7 domain (Chorley et al., 2012; Wang et al., 2013). In aryl hydrocarbon receptor signaling, NRF2 is often required for induction of classical AhR battery genes, e.g., by dioxin (Yeager et al., 2009). In xenobiotic metabolism signaling, NRF2 regulates genes encoding multiple drug-metabolizing enzymes (Pratt-Hyatt et al., 2013; Wu et al., 2012). In glutathione redox reactions, NRF2 regulates the enzymes that are responsible for regenerating and keeping glutathione in its reduced state (Hayes and Dinkova-Kostova, 2014). Finally, in glutathione biosynthesis, NRF2 regulates the expression of both subunits of the enzyme that catalyzes the rate-limiting step in glutathione biosynthesis (Moinova and Mulcahy, 1999). Moreover, MIND4 effects on gene transcription were confirmed to be translated into increased expression of NRF2-responsive proteins in both HD mutant and WT cells. Together, these results strongly implicate NRF2 as a central target of MIND4 activation.

The follow-up experiments with a close structural analog of MIND4, MIND4-17, suggested that the mechanism of NRF2 activation is SIRT2 independent. This conclusion was supported by results demonstrating similar effects of MIND4 and the known inducer SFP (Zhang et al., 1992) on the stabilization of NRF2 protein, a well-defined step in the pathway activation by NRF2 inducers. A functional study showed that MIND4 and MIND4-17, the latter lacking detectable SIRT2 inhibition activity, both reduce the production of ROS and reactive nitrogen intermediates (RNI) in microglia, consistent with the properties of NRF2 inducers. Together, these findings suggest that MIND4 and MIND4-17 represent a novel class of NRF2 activators.

(G) Concentration-dependent induction of the NRF2-responsive proteins NQO1 and GCLM in wild-type mouse cortical neurons (6 DIV) treated with MIND4 or MIND4-17 as indicated for 24 hr. Protein expression was detected by immunoblotting. Levels of α-tubulin were used as a loading control.

(H) Treatment of primary mouse corticostriatal co-cultures with 5 μM of MIND4-17-induced time-dependent increases in the transcriptional rate of a 5×-ARE promoter-luciferase reporter. *$p < 0.05$ by Student's t test with respect to DMSO-only controls.

(I–L) MIND4-17 induces concentration-dependent increases in transcription of the ARE genes *Nqo1* (I), *Hmox1* (J), *Gclc* (K), and *Srx1* (L) as quantified by qPCR. *$p < 0.05$ by Student's t test with respect to DMSO-only controls ("0").

(M and N) Similar concentration-dependent increases in the transcription of a 5×-ARE-luciferase reporter transfected into wild-type (light gray) versus mutant HD Q175/+ mouse neurons (black) in corticostriatal co-cultures were induced by treatment with MIND4 (M) and MIND4-17 (N) for 24 hr. *$p < 0.05$ by Student's t test with respect to DMSO-only controls ("0").

(O and P) Concentration-dependent induction by MIND4 (O) and MIND4-17 (P) of the NRF2-responsive NQO1 and GCLM proteins in primary mouse astroglia. Cultures were treated for 24 hr with MIND4 or MIND4-17 at the indicated concentrations. GFAP protein levels were used as a loading control.

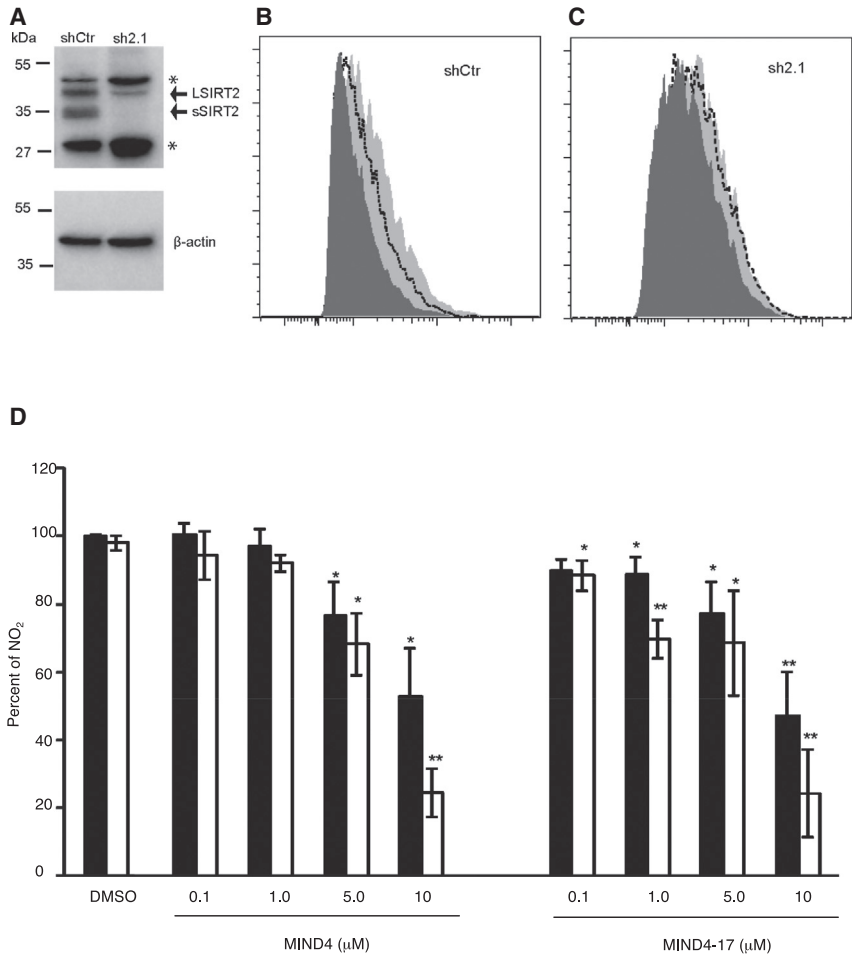

Figure 6. NRF2-Activating Properties of MIND4-17 in Microglia Cells with Intact or Knocked Down SIRT2 Protein

NRF2 activation properties were tested functionally by measuring the production of reactive oxygen species (ROS) and reactive nitrogen intermediates (RNI) in LPS/TNFα-induced microglia.

(A) N9 microglial cells were lentivirally transduced with shRNA for SIRT2 knock down (sh2.1) or with a scrambled control shRNA (shCtr). SIRT2 levels were detected by immunoblotting. Visualized SIRT2 non-specific SIRT2 bands are marked by *.

(B and C) ROS levels in stimulated microglia with intact SIRT2 (B) or after SIRT2 knockdown (C) treated with vehicle (DMSO), MIND4, or MIND4-17. Microglia cells were stimulated with LPS and TNF for 20 hr in medium supplemented with compounds at the indicated concentrations. Representative histograms of the fluorescence intensity for the ROS probe showing the overlays of vehicle (DMSO)-treated cells (filled light gray), treated with MIND4 (5 μM) (dotted line), or with MIND4-17 (2.5 μM) (filled dark gray).

(D) RNI production in stimulated microglia cells with functional SIRT2 (white bars) and SIRT2 knockdown (black bars). Cells were treated with vehicle (DMSO), MIND4, and MIND4-17 at the indicated concentrations. RNI was assessed by measurement of iNOS-dependent release of nitrites in the culture supernatants and quantified as percent of control (DMSO-treated cells). Data are presented as mean ± SD of four independent experiments. *$p < 0.05$ and **$p < 0.01$ by Student's t test.

The molecular mechanism of NRF2 activation was elucidated as targeting a cytoplasmic KEAP1 adapter protein through covalent modification of the major sensor-cysteine C151. That modification resulted in conformational change and arrest of the NRF2/KAEP1 complex, unable to target NRF2 for proteasome degradation, which leads to accumulation and nuclear translocation of de novo synthesized NRF2, and subsequent activation of ARE gene transcription. This NRF2 activation mechanism is described in depth in an accompanying manuscript.

Antioxidant activities mediated by the transcription factor NRF2 have emerged as a potential therapeutic approach to combat age-dependent neurodegeneration (Johnson et al., 2008; Joshi and Johnson, 2012; Tufekci et al., 2011; van Muiswinkel and Kuiperij, 2005; Xiong et al., 2015). Overexpression of NRF2 provides protection for primary neurons from expression of a mutant HTT fragment (Tsvetkov et al., 2013), and the efficacy of pharmacological activation of NRF2 has been shown in HD mice and is associated with induction of broad antioxidant effects in the brain (Ellrichmann et al., 2011; Stack et al., 2010).

SIGNIFICANCE

The discovery of a novel drug-like scaffold of thiazole-containing compounds as described here presents an opportunity to develop clinical lead candidates with distinct as well as combined/synergistic mechanisms of SIRT2 inhibition and/or NRF2 activation for treatment Huntington's disease and other neurodegenerative disorders.

EXPERIMENTAL PROCEDURES

All experimental procedures including the husbandry and sacrificing of animals were done in accordance with NIH guidelines and under Duke IACUC approval and oversight.

Compound Source and Storage

Compounds were procured from ChemBridge (purity QC ensured by provided NMR), dissolved in molecular-biology-grade DMSO from Sigma-Aldrich to 10 mM stock concentration, aliquoted, and stored at −80°C.

Characterization of Compound-Dependent Inhibition of SIRT2 Deacetylase Activity

Compound-dependent modulation of sirtuin activity was initially assessed using the Fluor de Lys fluorescent biochemical assay (BioMol) in a 96-well format as described previously (Outeiro et al., 2007). Deacetylation reaction was performed at 37°C for 1 hr in the presence of human recombinant enzymes: SIRT1 (BioMol-SE-239) 1 unit/per reaction, SIRT2 (BioMol-SE-251) 5 units/per reaction, or SIRT3 (BioMol-SE-270) 5 units/per reaction, compound of interest, standard buffer, 50 μM substrate, and 500 μM NAD^+ according to the manufacturer's protocol.

For analyzing the SIRT2 inhibition mechanism of MIND4 in a continuous coupled enzymatic assay with an α-tubulin peptide substrate, the recombinant enzyme was prepared and its activity analyzed as described previously

(Moniot et al., 2013). The IC_{50} for MIND4 was determined using α-tubulin and NAD^+ at 150 and 500 μM, respectively. The titration with NAD^+ was performed at 150 μM α-tubulin peptide, and peptide titration at 1 mM NAD^+. Data analysis and fitting was done in Grafit 7 (Erithacus Software).

Docking Model for Selective Binding of MIND4 to SIRT2

For generating the SIRT2/MIND4 complex model, the compound was docked using the program FlexX of the LeadIT suite (BioSolveIT) and a SIRT2/ADP-ribose structure (PDB: 3ZGV [Moniot et al., 2013]; ligand omitted for the calculation) as the receptor. The MIND4 molecule, generated as a 3D SDF file in MarvinSketch (ChemAxon), was docked with FlexX using default parameters, i.e., hybrid enthalpy and entropy-driven ligand binding, hard penalty on protein ligand clashes (maximum allowed overlap volume 3.2 $Å^3$), and average penalty on intra-ligand clashes (clash factor 0.6). The best pose was exported and visualized in PyMOL (Schrödinger LLC). The overlay with SIRT1 (PDB: 4KXQ) and with SIRT3 in complex with carba-NAD and acetylated peptide (PDB: 4FVT) was generated using the build-in align command of PyMOL.

NRF2 Stabilization Assay

COS1 cells were plated 16 hr before transfection. Cells were co-transfected with plasmids encoding WT KEAP1 and NRF2-V5 (generous gifts from Drs M. MacMahon and John D. Hayes, University of Dundee) at a 1:1 ratio. A plasmid encoding β-galactosidase was also transfected to monitor transfection efficiency. 24 hr post-transfection cells were exposed to MIND4 or sulforaphane for 24 hr, harvested, lysed, and extracts were prepared and loaded on SDS-PAGE normalized to β-gal expression activity. Samples were resolved on SDS-PAGE and immunoblotted with V5 antibody.

Rat Embryonic Striatal ST14A Cells

Compound bioactivity was tested in the rat embryonic striatal cell lines ST14A, which stably express either a mutant expanded repeat (128Q) or a WT (26Q) 546 amino acid HTT fragment (generous gift of E. Cattaneo) (Ehrlich et al., 2001). ST14A cells were propagated at 33°C in the presence of serum. To induce neuronal differentiation, cells were serum deprived and cultured at 37°C in the presence of N2 supplement (Invitrogen). Cells were treated with compounds for 24 hr, unless stated otherwise, as previously described (Quinti et al., 2010). Please see detailed information on antibodies and immunoblotting protocol in the Supplemental Experimental Procedures.

Microarray Data Analysis

RNA was extracted from HD mutant and WT ST14A cells, differentiated for 24 hr and treated with vehicle (DMSO) or with 5 μM MIND4, using the RNeasy Kit (QIAGEN). Labeled cRNAs were prepared and hybridized to Affymetrix GeneChip Rat Genome 230 2.0 microarrays according to the manufacturer's instructions. Affymetrix CEL (intensity) files from hybridized arrays were imported into the Partek Genome Suite (Partek Incorporated) for biostatistical analysis. 2 CEL files were used for each experimental condition: WT untreated, MIND4 treated (WT/MIND4), mutant (MTT) untreated, and mutant (MTT) MIND4-treated (MTT/MIND4). Two-way ANOVA was performed with interaction term included and evaluated to three contrasts of interest (cases I, II, and III). Gene lists were created for each of the three contrasts using the thresholds of absolute value of fold-change > 1.5 and a p value with false discovery rate < 0.05. The gene list included: for case I, 1765 genes; for case II, 1797 genes; and for case III, 268 genes, which were imported into Ingenuity IPA for pathway and network analyses. These analyses provided Networks (graph structures of molecules connected by relationships in the IPA knowledge base), Functions (lists of molecules grouped together due to their contribution to a biological function), and canonical pathways (molecules and relationships that participate in a biological pathway). Scores are assigned according to the probability that the genes from the user's list might appear in the function or pathway by chance (right-tailed Fisher's exact test).

Compound Tests in Acutely Transfected Rat Brain Slice Culture Assay

Coronal brain slices (250 μm thick) containing both cortex and striatum were prepared from CD Sprague-Dawley rat pups (Charles River) at postnatal day 10 and placed into an interface culture as previously described (Reinhart et al., 2011). A biolistic device (Helios Gene Gun; Bio-Rad) was used to co-transfect the brain slices with a yellow fluorescent protein (YFP) visual reporter and a mutant HTT plasmid containing human HTT exon-1 harboring a 73 CAG repeat to induce neurodegeneration of medium spiny neurons (MSNs). MIND4 and a positive control, the pan-caspase inhibitor Boc-D-FMK (Sigma-Aldrich) at 100 μM (Varma et al., 2007), were added to culture wells at the time of slice preparation. YFP co-transfected MSNs were identified 4 days after incubation by their location within the striatum and by their characteristic dendritic arborization as previously described (Crittenden et al., 2010; Reinhart et al., 2011). Please see Supplemental Experimental Procedures for detailed protocol and analysis.

Transcriptional Assays in Primary Corticostriatal Neuronal Co-cultures

Primary corticostriatal neuronal co-cultures were prepared from E18 WT or Q175/+ (Menalled et al., 2012) mouse brains as previously described (Kaltenbach et al., 2010). For 5×-ARE-luciferase reporter assays, neurons were transfected with 2.5 μg Cignal Antioxidant Response Reporter dual luciferase plasmids (Qiagen/SABiosciences). For qRT-PCR of ARE target genes, corticostriatal co-cultures were prepared as described (Kaltenbach et al., 2010) and after 4 days in culture treated for 6 hr with the indicated compounds followed by RNA harvesting. Please see Supplemental Experimental Procedures for detailed protocol. C_t values were determined using primer sets against ARE genes *Hmox1*, *Srx*, *Gclc*, and *Nqo1* (Yang et al., 2012). Each sample was run in technical triplicate and relative expression expressed as fold-change over control after normalizing each sample to C_t values for GAPDH.

Compound Tests in a *Drosophila* Model of HD

Treatment of a *Drosophila* HD model with compound and efficacy analysis of the effects of MIND4 on photoreceptor neurons was performed as previously described (Pallos et al., 2008). The indicated numbers of flies were scored for each condition (n) with the number of ommatidia scored indicated in parentheses. Trial 1: DMSO = 11(449); MIND4 1 μM = 3(112); MIND4 10 μM = 9(337); MIND4 30 μM = 9(364). Trial 2: DMSO = 8(361); MIND4 10 μM = 8(292). Relative rescue of photoreceptor neurons in flies treated versus untreated with MIND4 at 10 μM dose was estimated for trial 1 and trial 2 as 22.6% and 20.7%, respectively; t test significance for trial 1 was $p < 0.001$ and for trial 2 was $p < 0.02$.

Compound Tests Using ROS/RNI Assays in Stimulated Microglia Cells

N9 microglial cells lentiviral transduced with shRNA for SIRT2 knockdown or with a scrambled control shRNA were cultured in RPMI medium containing GlutaMAX (Invitrogen) and supplemented with 10% fetal bovine serum (endotoxin levels lower than 10 EU/ml). Cells were plated in 96-well plates (5×10^4/well) and cultured overnight before stimulation with LPS (100 ng/ml) and TNF (10 ng/ml) for 20 hr in medium supplemented with DMSO or with the tested compounds. ROS levels were detected by flow cytometry after microglia incubation with 10 μM 5-(and-6)-chloromethyl-2′,7′-dichlorodihydrofluorescein diacetate acetyl ester (CM-H_2DCFDA) (Invitrogen) for 20 min. The production of nitric oxide by iNOS was measured indirectly by assaying nitrites in the culture supernatant using the Griess reaction. Briefly, 100 μl of supernatants was incubated with an equal amount of Griess reagent (1% sulfanilamide, 0.1% naphthylethylenediamine in 2% phosphoric acid solution) and the absorbance read at 550 nm after 20 min of incubation at room temperature.

SUPPLEMENTAL INFORMATION

Supplemental Information includes Supplemental Experimental Procedures, one figure, and two tables and can be found with this article online at http://dx.doi.org/10.1016/j.chembiol.2016.05.015.

AUTHOR CONTRIBUTIONS

L.Q. conducted identification, characterization, and analysis of compound properties, and was involved in manuscript preparation; D.L. and N.A.R. assisted with in vitro experiments; M.M.M. supervised compound characterization studies in primary neurons and astroglia; M.C. performed IPA and identified NRF2 activation property of MIND4, R.G.L. assisted with gene expression analysis; J.E.L. performed the microarray experiment and assisted with

analysis; H.R. and R.L.C. performed microarray analysis in primary neurons; A.D.K. and S.D.N. planned and performed the experiments in NRF2 stabilization, A.D.K. participated in writing and editing of the manuscript; T.F.P. tested compound effects on ROS/RNI in microglia; M.J.V.K. performed compound NRF2 transcriptional profiling in primary neuronal cultures, L.S.K. tested MIND4 in brain slices; D.C.L. supervised the experiments, analyzed the data, and edited the manuscript; J.P and J.L.M. were involved in the *Drosophila* studies; J.L.M. edited the manuscript; S.M. and C.S. characterized compound SIRT2 inhibition activity, assisted by L.M.; C.S. edited the manuscript; E.S. analyzed the compound structures and provided chemistry expertise; R.B. performed the docking and modeling studies; L.M.T. was involved in planning transcriptional studies, data analysis, and manuscript preparation; A.G.K. planned, organized, and was involved in data mining and analysis, manuscript writing, and preparation. L.Q., M.C., and S.M. contributed equally to the work.

ACKNOWLEDGMENTS

This work was supported by grants from the NIH U01-NS066912, R01NS04528, NIH NS078370, NIH NS080514, and NIGMS grant GM080356, the Biotechnology and Biological Sciences Research Council (BB/J007498/1, BB/L01923X/1), Alzheimer Forschung Initiative (grant 14834 to C.S.) and Cancer Research UK (C20953/A18644). We also acknowledge support from the RJG foundation to L.Q and A.G.K and from the American Heart Association to R.G.L. This work was made possible in part by the availability of the Optical Biology Shared Resource of the Cancer Center Support Grant (CA-62203) at the University of California, Irvine. We thank Michael McMahon (University of Dundee) for plasmids encoding wild-type Keap1.

Received: September 28, 2015
Revised: April 26, 2016
Accepted: May 17, 2016
Published: July 14, 2016

REFERENCES

(1993). A novel gene containing a trinucleotide repeat that is expanded and unstable on Huntington's disease chromosomes. The Huntington's Disease Collaborative Research Group. Cell *72*, 971–983.

Aguilera, P., Chanez-Cardenas, M.E., Floriano-Sanchez, E., Barrera, D., Santamaria, A., Sanchez-Gonzalez, D.J., Perez-Severiano, F., Pedraza-Chaverri, J., and Jimenez, P.D. (2007). Time-related changes in constitutive and inducible nitric oxide synthases in the rat striatum in a model of Huntington's disease. Neurotoxicology *28*, 1200–1207.

Browne, S.E., and Beal, M.F. (2006). Oxidative damage in Huntington's disease pathogenesis. Antioxid. Redox Signal. *8*, 2061–2073.

Chopra, V., Quinti, L., Kim, J., Vollor, L., Narayanan, K.L., Edgerly, C., Cipicchio, P.M., Lauver, M.A., Choi, S.H., Silverman, R.B., et al. (2012). The sirtuin 2 inhibitor AK-7 is neuroprotective in Huntington's disease mouse models. Cell Rep. *2*, 1492–1497.

Chorley, B.N., Campbell, M.R., Wang, X., Karaca, M., Sambandan, D., Bangura, F., Xue, P., Pi, J., Kleeberger, S.R., and Bell, D.A. (2012). Identification of novel NRF2-regulated genes by ChIP-seq: influence on retinoid X receptor alpha. Nucleic Acids Res. *40*, 7416–7429.

Crittenden, J.R., Dunn, D.E., Merali, F.I., Woodman, B., Yim, M., Borkowska, A.E., Frosch, M.P., Bates, G.P., Housman, D.E., Lo, D.C., et al. (2010). CalDAG-GEFI down-regulation in the striatum as a neuroprotective change in Huntington's disease. Hum. Mol. Genet. *19*, 1756–1765.

Crook, Z.R., and Housman, D. (2011). Huntington's disease: can mice lead the way to treatment? Neuron *69*, 423–435.

Ehrlich, M.E., Conti, L., Toselli, M., Taglietti, L., Fiorillo, E., Taglietti, V., Ivkovic, S., Guinea, B., Tranberg, A., Sipione, S., et al. (2001). ST14A cells have properties of a medium-size spiny neuron. Exp. Neurol. *167*, 215–226.

Ellrichmann, G., Petrasch-Parwez, E., Lee, D.H., Reick, C., Arning, L., Saft, C., Gold, R., and Linker, R.A. (2011). Efficacy of fumaric acid esters in the R6/2 and YAC128 models of Huntington's disease. PLoS One *6*, e16172.

Hayes, J.D., and Dinkova-Kostova, A.T. (2014). The Nrf2 regulatory network provides an interface between redox and intermediary metabolism. Trends Biochem. Sci. *39*, 199–218.

Innamorato, N.G., Rojo, A.I., Garcia-Yague, A.J., Yamamoto, M., de Ceballos, M.L., and Cuadrado, A. (2008). The transcription factor Nrf2 is a therapeutic target against brain inflammation. J. Immunol. *181*, 680–689.

Johnson, J.A., Johnson, D.A., Kraft, A.D., Calkins, M.J., Jakel, R.J., Vargas, M.R., and Chen, P.C. (2008). The Nrf2-ARE pathway: an indicator and modulator of oxidative stress in neurodegeneration. Ann. N Y Acad. Sci. *1147*, 61–69.

Johri, A., and Beal, M.F. (2012). Antioxidants in Huntington's disease. Biochim. Biophys. Acta *1822*, 664–674.

Joshi, G., and Johnson, J.A. (2012). The Nrf2-ARE pathway: a valuable therapeutic target for the treatment of neurodegenerative diseases. Recent Pat. CNS Drug Discov. *7*, 218–229.

Kaltenbach, L.S., Bolton, M.M., Shah, B., Kanju, P.M., Lewis, G.M., Turmel, G.J., Whaley, J.C., Trask, O.J., Jr., and Lo, D.C. (2010). Composite primary neuronal high-content screening assay for Huntington's disease incorporating non-cell-autonomous interactions. J. Biomol. Screen *15*, 806–819.

Koh, K., Kim, J., Jang, Y.J., Yoon, K., Cha, Y., Lee, H.J., and Kim, J. (2011). Transcription factor Nrf2 suppresses LPS-induced hyperactivation of BV-2 microglial cells. J. Neuroimmunol. *233*, 160–167.

Li, X., Valencia, A., Sapp, E., Masso, N., Alexander, J., Reeves, P., Kegel, K.B., Aronin, N., and Difiglia, M. (2010). Aberrant Rab11-dependent trafficking of the neuronal glutamate transporter EAAC1 causes oxidative stress and cell death in Huntington's disease. J. Neurosci. *30*, 4552–4561.

Liu, L., Arun, A., Ellis, L., Peritore, C., and Donmez, G. (2013). Sirtuin 2 (SIRT2) enhances 1-methyl-4-phenyl-1,2,3,6-tetrahydropyridine (MPTP)-induced nigrostriatal damage via deacetylating forkhead box O3a (Foxo3a) and activating Bim protein. J. Biol. Chem. *287*, 32307–32311.

Luthi-Carter, R., Hanson, S.A., Strand, A.D., Bergstrom, D.A., Chun, W., Peters, N.L., Woods, A.M., Chan, E.Y., Kooperberg, C., Krainc, D., et al. (2002). Dysregulation of gene expression in the R6/2 model of polyglutamine disease: parallel changes in muscle and brain. Hum. Mol. Genet. *11*, 1911–1926.

Luthi-Carter, R., Taylor, D.M., Pallos, J., Lambert, E., Amore, A., Parker, A., Moffitt, H., Smith, D.L., Runne, H., Gokce, O., et al. (2010). SIRT2 inhibition achieves neuroprotection by decreasing sterol biosynthesis. Proc. Natl. Acad. Sci. USA *107*, 7927–7932.

Marsh, J.L., Pallos, J., and Thompson, L.M. (2003). Fly models of Huntington's disease. Hum. Mol. Genet. *12 Spec No 2*, R187–R193.

Maxwell, M.M., Tomkinson, E.M., Nobles, J., Wizeman, J.W., Amore, A.M., Quinti, L., Chopra, V., Hersch, S.M., and Kazantsev, A.G. (2011). The Sirtuin 2 microtubule deacetylase is an abundant neuronal protein that accumulates in the aging CNS. Hum. Mol. Genet. *20*, 3986–3996.

McMahon, M., Lamont, D.J., Beattie, K.A., and Hayes, J.D. (2010). Keap1 perceives stress via three sensors for the endogenous signaling molecules nitric oxide, zinc, and alkenals. Proc. Natl. Acad. Sci. USA *107*, 18838–18843.

Menalled, L.B., Kudwa, A.E., Miller, S., Fitzpatrick, J., Watson-Johnson, J., Keating, N., Ruiz, M., Mushlin, R., Alosio, W., McConnell, K., et al. (2012). Comprehensive behavioral and molecular characterization of a new knock-in mouse model of Huntington's disease: zQ175. PLoS One *7*, e49838.

Moinova, H.R., and Mulcahy, R.T. (1999). Up-regulation of the human gamma-glutamylcysteine synthetase regulatory subunit gene involves binding of Nrf-2 to an electrophile responsive element. Biochem. Biophys. Res. Commun. *261*, 661–668.

Moller, T. (2010). Neuroinflammation in Huntington's disease. J. Neural Transm. *117*, 1001–1008.

Moniot, S., Schutkowski, M., and Steegborn, C. (2013). Crystal structure analysis of human Sirt2 and its ADP-ribose complex. J. Struct. Biol. *182*, 136–143.

North, B.J., Marshall, B.L., Borra, M.T., Denu, J.M., and Verdin, E. (2003). The human Sir2 ortholog, SIRT2, is an NAD+-dependent tubulin deacetylase. Mol. Cell *11*, 437–444.

Outeiro, T.F., Kontopoulos, E., Altmann, S.M., Kufareva, I., Strathearn, K.E., Amore, A.M., Volk, C.B., Maxwell, M.M., Rochet, J.C., McLean, P.J., et al. (2007). Sirtuin 2 inhibitors rescue alpha-synuclein-mediated toxicity in models of Parkinson's disease. Science *317*, 516–519.

Pais, T.F., Szego, E.M., Marques, O., Miller-Fleming, L., Antas, P., Guerreiro, P., de Oliveira, R.M., Kasapoglu, B., and Outeiro, T.F. (2013). The NAD-dependent deacetylase sirtuin 2 is a suppressor of microglial activation and brain inflammation. EMBO J. *32*, 2603–2616.

Pallos, J., Bodai, L., Lukacsovich, T., Purcell, J.M., Steffan, J.S., Thompson, L.M., and Marsh, J.L. (2008). Inhibition of specific HDACs and sirtuins suppresses pathogenesis in a Drosophila model of Huntington's disease. Hum. Mol. Genet. *17*, 3767–3775.

Pratt-Hyatt, M., Lickteig, A.J., and Klaassen, C.D. (2013). Tissue distribution, ontogeny, and chemical induction of aldo-keto reductases in mice. Drug Metab. Dispos. *41*, 1480–1487.

Quintanilla, R.A., and Johnson, G.V. (2009). Role of mitochondrial dysfunction in the pathogenesis of Huntington's disease. Brain Res. Bull. *80*, 242–247.

Quinti, L., Chopra, V., Rotili, D., Valente, S., Amore, A., Franci, G., Meade, S., Valenza, M., Altucci, L., Maxwell, M.M., et al. (2010). Evaluation of histone deacetylases as drug targets in Huntington's disease models. Study of HDACs in brain tissues from R6/2 and CAG140 knock-in HD mouse models and human patients and in a neuronal HD cell model. PLoS Curr. *2*.

Rauh, D., Fischer, F., Gertz, M., Lakshminarasimhan, M., Bergbrede, T., Aladini, F., Kambach, C., Becker, C.F., Zerweck, J., Schutkowski, M., et al. (2013). An acetylome peptide microarray reveals specificities and deacetylation substrates for all human sirtuin isoforms. Nat. Commun. *4*, 2327.

Reinhart, P.H., Kaltenbach, L.S., Essrich, C., Dunn, D.E., Eudailey, J.A., DeMarco, C.T., Turmel, G.J., Whaley, J.C., Wood, A., Cho, S., et al. (2011). Identification of anti-inflammatory targets for Huntington's disease using a brain slice-based screening assay. Neurobiol. Dis. *43*, 248–256.

Sorolla, M.A., Rodriguez-Colman, M.J., Vall-llaura, N., Tamarit, J., Ros, J., and Cabiscol, E. (2012). Protein oxidation in Huntington disease. Biofactors *38*, 173–185.

Stack, C., Ho, D., Wille, E., Calingasan, N.Y., Williams, C., Liby, K., Sporn, M., Dumont, M., and Beal, M.F. (2010). Triterpenoids CDDO-ethyl amide and CDDO-trifluoroethyl amide improve the behavioral phenotype and brain pathology in a transgenic mouse model of Huntington's disease. Free Radic. Biol. Med. *49*, 147–158.

Steffan, J.S., Bodai, L., Pallos, J., Poelman, M., McCampbell, A., Apostol, B.L., Kazantsev, A., Schmidt, E., Zhu, Y.Z., Greenwald, M., et al. (2001). Histone deacetylase inhibitors arrest polyglutamine-dependent neurodegeneration in Drosophila. Nature *413*, 739–743.

Taylor, D.M., Maxwell, M.M., Luthi-Carter, R., and Kazantsev, A.G. (2008). Biological and potential therapeutic roles of sirtuin deacetylases. Cell Mol. Life Sci. *65*, 4000–4018.

Tsunemi, T., Ashe, T.D., Morrison, B.E., Soriano, K.R., Au, J., Roque, R.A., Lazarowski, E.R., Damian, V.A., Masliah, E., and La Spada, A.R. (2012). PGC-1alpha rescues Huntington's disease proteotoxicity by preventing oxidative stress and promoting TFEB function. Sci. Transl. Med. *4*, 142ra197.

Tsvetkov, A.S., Arrasate, M., Barmada, S., Ando, D.M., Sharma, P., Shaby, B.A., and Finkbeiner, S. (2013). Proteostasis of polyglutamine varies among neurons and predicts neurodegeneration. Nat. Chem. Biol. *9*, 586–592.

Tufekci, K.U., Civi Bayin, E., Genc, S., and Genc, K. (2011). The Nrf2/are pathway: a promising target to counteract mitochondrial dysfunction in Parkinson's disease. Parkinsons Dis. *2011*, 314082.

van Muiswinkel, F.L., and Kuiperij, H.B. (2005). The Nrf2-ARE Signalling pathway: promising drug target to combat oxidative stress in neurodegenerative disorders. Curr. Drug Targets *4*, 267–281.

Varma, H., Cheng, R., Voisine, C., Hart, A.C., and Stockwell, B.R. (2007). Inhibitors of metabolism rescue cell death in Huntington's disease models. Proc. Natl. Acad. Sci. USA *104*, 14525–14530.

Wang, H., Liu, K., Geng, M., Gao, P., Wu, X., Hai, Y., Li, Y., Li, Y., Luo, L., Hayes, J.D., et al. (2013). RXRalpha inhibits the NRF2-ARE signaling pathway through a direct interaction with the Neh7 domain of NRF2. Cancer Res. *73*, 3097–3108.

Wu, K.C., Cui, J.Y., and Klaassen, C.D. (2012). Effect of graded Nrf2 activation on phase-I and -II drug metabolizing enzymes and transporters in mouse liver. PLoS One *7*, e39006.

Xiong, W., MacColl Garfinkel, A.E., Li, Y., Benowitz, L.I., and Cepko, C.L. (2015). NRF2 promotes neuronal survival in neurodegeneration and acute nerve damage. J. Clin. Invest. *125*, 1433–1445.

Yang, B., Fu, J., Zheng, H., Xue, P., Yarborough, K., Woods, C.G., Hou, Y., Zhang, Q., Andersen, M.E., and Pi, J. (2012). Deficiency in the nuclear factor E2-related factor 2 renders pancreatic beta-cells vulnerable to arsenic-induced cell damage. Toxicol. Appl. Pharmacol. *264*, 315–323.

Yeager, R.L., Reisman, S.A., Aleksunes, L.M., and Klaassen, C.D. (2009). Introducing the "TCDD-inducible AhR-Nrf2 gene battery". Toxicol. Sci. *111*, 238–246.

Zhang, Y., Talalay, P., Cho, C.G., and Posner, G.H. (1992). A major inducer of anticarcinogenic protective enzymes from broccoli: isolation and elucidation of structure. Proc. Natl. Acad. Sci. USA *89*, 2399–2403.